

Calculations of impact stresses in polycrystalline graphite rods

M. I. DARBY

Department of Pure and Applied Physics, University of Salford, Salford, Lancashire, UK

Calculations have been made to determine the maximum stresses produced in polycrystalline graphite rod specimens by a single impact of an anvil. The method of Timoshenko was employed, which combines the vibrational theory of Bernoulli with Hertz's theory of impact. The deformation parameter in the Hertz theory was obtained by fitting experimental results for the impact force as a function of time, and was found to be appreciably larger than values calculated from linear elastic theory. The model was unable to account for the energy losses observed experimentally. The predicted peak stresses corresponding to experimental conditions of single impact failure correlated well with the three-point bend strengths of the types of graphite considered.

1. Introduction

The impact properties of polycrystalline graphite rods have recently been studied experimentally by Birch and Brocklehurst [1, 2]. An anvil was allowed to strike the specimen repeatedly with constant energy until fracture occurred, and the resulting endurance curves were interpreted using a fracture mechanic approach [3]. The variation of the impact force on a rod as a function of time was also measured, and from it the maximum stresses at failure were estimated using a static load stress formula. The experimental data quoted in this paper arises from the studies of Birch and Brocklehurst [1, 2].

To obtain an understanding of the impact failure mechanism, it is necessary to be able to make the best calculations of the maximum stresses produced in a specimen by a single impact. The aim of the theoretical work reported here was to investigate how important the vibrational response of the specimen is in determining the stresses. The well known method of Timoshenko [4, 5] was employed, which combines the Bernoulli vibrational theory for a beam with Hertz theory for the impact force. As will be seen, its application to impact in graphite rods was not straightforward.

In the tests of Birch and Brocklehurst [1, 2], cylindrical beam specimens, typically of length

120 mm and radius 7.5 mm, were simply supported horizontally by suitable holders at each end, and were struck half-way along their length by an anvil attached to a pendulum. The striking surface of the anvil was usually cylindrical, with its axis perpendicular to the beam, having a radius of curvature of approximately 2 mm, and the area of contact with the specimen was very small. The velocity of the anvil at the point of impact was varied by adjusting the height of release of the pendulum, and was measured using a non-contacting displacement transducer. The effective mass of the anvil was estimated from measurements of the moment of inertia of the pendulum.

2. Theory

In calculating the stresses in a specimen subjected to an impulsive force, it was necessary to make a number of basic initial simplifying assumptions:

1. the specimens have linear, isotropic elastic properties;
2. a theory of Hertz [6, 7] for perfectly elastic bodies provides an adequate description of the deformations of the anvil and the specimen;
3. no energy is lost to the specimen supports, or to other parts of the testing machinery.

It is well known [8] that the constitutive relation for polycrystalline graphite is not linear and, moreover, a permanent set can be produced

by an applied stress. However, it was impracticable to include these effects on the response of the specimen, or on the deformation process.

Further, it was not possible to account for the energy losses to the machinery, although such losses will be important in the experiments [9], and need to be estimated before a comparison can be made between theory and experiment.

The equation for the deflection, w , of a beam performing transverse vibrations under the application of a force $F(\mathbf{r}, t)$ dependent on position \mathbf{r} and time t is [8]

$$D\nabla_w^4 + \rho_a \frac{\partial^2 w}{\partial t^2} = F(\mathbf{r}, t) \quad (1)$$

where D and ρ_a are appropriate constants. In impact experiments the force F is impulsive, being finite for a time typically of order 1 msec. If the thickness of the specimen is not small compared with the other dimensions, a number of corrections [5] must be added to Equation 1. A more important omission in Equation 1 is the effect of damping, which introduces a term in $\partial w/\partial t$. Unfortunately, solutions of the modified homogeneous equation become so complex [10, 11] that progress on the impact problem is very difficult. Since the ends of the beam are simply supported, the boundary conditions on Equation 1 are that $w = 0$ and $\partial^2 w/\partial x^2 = 0$ at the ends, where x is the axial coordinate.

For perfectly elastic bodies, Hertz [6, 7] has shown that the depth of the indentation in the specimen, α , produced by an impactor is proportional to $F^{2/3}$:

$$\alpha = kF^{2/3}(t) \quad (2)$$

where k depends on the elastic constants of the two bodies and the geometries of the contacting surfaces. Assuming that impact occurs at a point $\mathbf{r} = \mathbf{r}_i$ on the specimen, and denoting by w_0 the displacement of the impactor's point of contact after time t , and by $w(\mathbf{r}_i, t)$ the displacement of the face of the specimen, then by definition

$$\alpha = w_0 - w(\mathbf{r}_i, t) \quad (3)$$

If v_0 is the impact velocity of the impactor, and m its mass, Equations 2 and 3 can be combined to give the following integral equation for the impulsive force function:

$$kF^{2/3}(t) = v_0 t - \frac{1}{m} \int_0^t dt \int_0^t F(t') dt' - w(\mathbf{r}_i, t) \quad (4)$$

The force function $F(t)$ and the specimen deflection can be calculated, therefore, from the coupled Equations 1 and 4.

For the transverse impact of an anvil at the centre of a beam, length L , simply supported at both ends, the beam can be considered to be one-dimensional. The normal modes of free vibration, X_i , are just [12]:

$$X_i(x) = \sin\left(\frac{i\pi x}{L}\right) \quad (5)$$

Seeking a solution of Equation (1) in the form

$$w(x, t) = \sum_{i=1}^{\infty} q_i(t) X_i(x) \quad (6)$$

the Lagrange's equation for the $q_i(t)$ is

$$\frac{\partial^2 q}{\partial t^2} + \omega_i^2 q_i = \frac{F(t) X_i(L/2)}{\rho_a \int_0^L X_i^2 dx} = \frac{2F(t)}{\rho_a L} \quad (7)$$

where

$$\omega_i = \left(\frac{i\pi c}{L}\right)^2 \quad (8)$$

$$c^2 = \left(\frac{EI}{\rho A}\right)^{1/2} \quad (9)$$

and A is the cross-sectional area. In the notation of Equation 1, $D = EI$ and $\rho_a = \rho A$, the mass per unit length; ρ is the density and E is Young's modulus.

Solving Equation 7 yields for the displacement:

$$w(x, t) = \sum_{i \text{ odd}} \left[\frac{2}{\rho_a L \omega_i} \times \left\{ \int_0^t F(t') \sin \omega_i(t-t') dt' \right\} \sin\left(\frac{i\pi x}{L}\right) \right] \quad (10)$$

assuming that the initial displacement and velocity of the beam are zero. Employing Equation 10 in Equation 4, with $x = L/2$ the integral equation for $F(t)$ becomes

$$kF^{2/3}(t) = v_0 t - \frac{1}{m} \int_0^t (t-t') F(t') dt' - \frac{2}{A \rho L} \sum_{i \text{ odd}} \left\{ \frac{1}{\omega_i} \int_0^t F(t') \times \sin \left[\left(\frac{i\pi c}{L}\right)^2 (t-t') \right] dt' \right\}. \quad (11)$$

This equation can only be solved numerically.

It is clear from Equation 11 that the Hertz constant, k , plays an important role in determining the function $F(t)$. It contains all the information about the geometry and elastic properties of the anvil, and also depends on the geometry and elastic properties of the specimen.

Hertz [6] considered the conditions of contact of two perfectly elastic bodies with ellipsoidal surfaces which have symmetry about a direction, the z -axis, perpendicular to the plane of contact. He showed that the area where contact is made is elliptical, and is displaced from the initial position in the $z = 0$ plane by a distance α given by:

$$\alpha = \frac{3}{4a} P(I_1 + I_2) I_\alpha \quad (12)$$

where P = contact pressure

$$I_i = \frac{(1 - \nu_i)^2}{\pi E_i} \quad (i = 1, 2) \quad (13)$$

$$I_\alpha = \int_0^\infty \frac{ds}{[s(1+s)(1-e^2+s)]^{1/2}} \quad (14)$$

a = major axis of compressed area

$$= \left\{ \frac{3}{4A} P(I_1 + I_2) I_\alpha \right\}^{1/3} \quad (15)$$

e = ellipticity of compressed area

$$I_a = \int_0^\infty \frac{ds}{(1+s)^{3/2} [s(1-e^2+s)]^{1/2}} \quad (16)$$

A' = average curvature of the bodies in the x z -plane before contact

It follows from Equations 12 and 15 that α is proportional to $P^{2/3}$

$$\alpha = kP^{2/3} \quad (17)$$

where the Hertz constant, k is given by

$$k = \left[\frac{I_\alpha}{A' \left(\frac{3}{4}\right)^2 (I_1 + I_2)^2 I_a^3} \right]^{-1/3} \quad (18)$$

It should be noted that Hertz [6] used a different constant, k_2 , given by

$$k_2 = k^{-3/2} \quad (19)$$

As would be expected, it can be seen from Equations 13 and 18 that the smaller the values of the Young's moduli, the larger is the deformation for a given force. In employing Equation 18, the ellipticity, e , was obtained using tabulated results given by Love [7].

3. Numerical calculations

Equation 11 for the impact force contains a sum of time integrals involving $F(t)$, and generally the integral equation can only be solved numerically. The methods commonly employed [4, 12] use finite time elements and an iteration process. The force is determined at times, t , given by $t = j\Delta t$, where j is an integer and Δt is a small time increment.

It is important in iterative methods to have good starting approximations. The force function was chosen to be of sinusoidal form [13]:

$$F(t) = \begin{cases} F_0 \sin\left(\frac{\pi t}{t_c}\right) & (t \leq t_c) \\ 0 & (\text{otherwise}) \end{cases} \quad (20)$$

with F_0 and t_c as parameters. An approximate values of t_c , the time of contact, was obtained from Hertz's theory [7]:

$$t_c = \frac{2.9432}{v_0} \left(\frac{5}{k_1 k_2}\right)^{2/5} \left(\frac{v_0}{2}\right)^{4/5} \quad (21)$$

where

$$k_1 = (m_1 + m_2)/m_1 m_2 \quad (22)$$

and k_2 is given by Equation 19. For an anvil of mass $m_1 = 0.2$ kg striking a beam of mass $m_2 = 0.05$ kg, with $v_0 = 1$ m sec⁻¹, and $k_2 \approx 10^9$ N m^{-3/2}, Equation 21 gives $t_c \approx 3.5$ msec.

A zero order treatment of the impact problem for a beam by Timoshenko and Young [5] provide useful estimates of the maximum impact force. Equating the kinetic energy lost by the impactor with the potential energy gained by the deformed beam,

$$F_0 \approx v_0 \left(\frac{48EI m}{L^3}\right)^{1/2} \quad (23)$$

For a cylindrical beam of radius r , $I = 0.25\pi r^4$, and taking $E = 1.1 \times 10^{10}$ N m⁻², $r = 7.5 \times 10^{-3}$, $L = 0.12$ m, $m = 0.5$ kg, Equation 23 yields for $v_0 = 1.0$ m sec⁻¹

$$F_0 \approx 600 \text{ N}$$

for a typical graphite beam.

The starting parameters F_0 and t_c chosen on this basis were usually taken to be $F_0 = 800$ (N) and $t_c = 2$ (msec). These values were not critical and, for example, the choices $F_0 = 400$ (N), $t_c = 1$ (msec) or $F_0 = 800$ (N), $t_c = 5$ (msec) were equally satisfactory.

The time increment used was taken to be $\Delta t = t_c/300$. Decreasing Δt below this value did not improve the solution for the cases tested. The

total time of integration was arbitrarily chosen to be $2t_c$. After each iteration, the function $F(t)$ was set equal to zero at times, greater than t_d say, when the calculated values were negative. The quantity, t_d , was the contact time for the impact. In all cases tested it was found that $t_d < 2t_c$, but had this not been so, the upper limit of $2t_c$ would have had to be increased. It was found that of order 50 iterations were required to obtain solutions accurate to better than $1:10^6$. The sum over vibrational modes in the integral Equation 11 converges rapidly and the sum was typically terminated after ten terms.

The displacements and stresses in a specimen as functions of time are readily calculated, in principle, from a knowledge of $F(t)$. However, the time integrals involved, of the form

$$I(t) = \int_0^t F(t') \sin \omega(t-t') dt' \quad (24)$$

are often difficult to evaluate numerically, particularly when $F(t)$ shows oscillatory features, and it was found convenient to represent $F(t)$ as a Fourier series in the time interval $0 < t < t_d$, where t_d is the duration of the pulse

$$F(t) = \begin{cases} \sum_{n=1}^N F_n \sin(n\beta t) & (0 \leq t \leq t_d) \\ 0 & (t > t_d) \end{cases} \quad (25)$$

with

$$\beta = \pi/t_d \quad (27)$$

The coefficients F_n are determined from $F(t)$ employing

$$F_n = \frac{2}{t_d} \int_0^{t_d} F(t) \sin(n\beta t) dt \quad (28)$$

Substituting Equations 25 and 28 into Equation 24, and defining

$$t_0 = \begin{cases} t & (t \leq t_d) \\ t_d & (t > t_d) \end{cases} \quad (29)$$

yields

$$I(t) = \frac{1}{t_d} \sum_{n=1}^N F_n \left\{ \sin \omega t \left[\frac{1 - \cos(n\beta + \omega)t_0}{n\beta + \omega} - \frac{1 - \cos(n\beta - \omega)t_0}{n\beta - \omega} \right] - \cos \omega t \left[\frac{\sin(n\beta - \omega)t_0}{n\beta - \omega} - \frac{\sin(n\beta + \omega)t_0}{n\beta + \omega} \right] \right\} \quad (30)$$

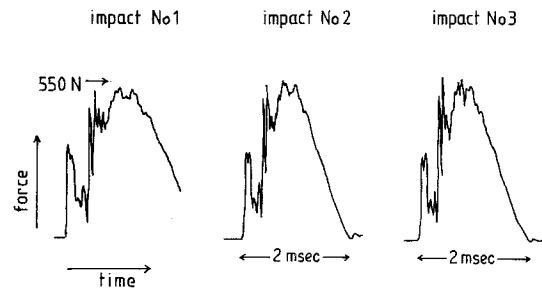


Figure 1 Typical experimental impact force curves for a gilsocarbon beam.

The number of terms N required in the series depends on the complexity of $F(t)$, but in practice an upper limit of 10 was set for its value.

4. Results

Measurements of the impact force as a function of time were made by Birch and Brocklehurst [2] using a force transducer behind the anvil head. Typical curves obtained for $F(t)$ are shown in Fig. 1, and the physical properties in the symmetry direction for some of the tested graphites are given in Table I.

It was found that the shape of $F(t)$ varied slightly with the number of previous impacts received by a beam, the greatest difference being between the first and second impacts, presumably due to bedding down of various parts of the experimental arrangement. The present theory is, of course, unable to account for such variations.

Experiments on Gilsocarbon beams were made using anvils with both spherical and cylindrical surfaces, and it was of interest to determine theoretically what difference, if any, the anvil geometry had on the predicted force functions. In both cases, the radii of curvature of the anvil faces were approximately 2 mm, and a straightforward evaluation of Equation 18 gave values of the Hertz constants.

TABLE I Properties of graphite specimens considered

Graphite	Bulk density (kg m ⁻³)	Dynamic Young's modulus* (GN m ⁻²)	Three-point bend strength* (MN m ⁻²)
PGA	1699	11.5	16.4
EY9	1660	6.4	25.8
Gilsocarbon	1805	11.4	44.0
POCO	1860	12.0/14.8	96.0

*Values parallel to the symmetry axis.

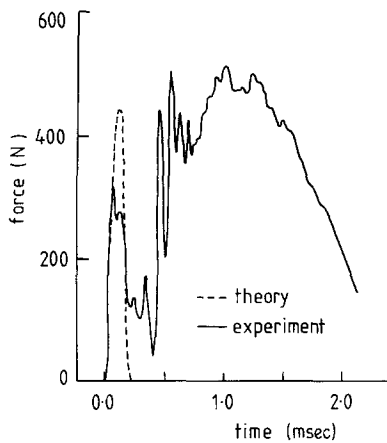


Figure 2 Impact force function for a gilsocarbon beam; (length 99 mm, radius 7.5 mm, impactor mass 0.289 kg, impact velocity 1.31 m sec^{-1}). *Ab initio* Hertz constant used in theory.

$$k = 1.205 \times 10^{-6} \text{ m N}^{-2/3} \quad \text{cyl. anvil} \quad (31)$$

$$k = 1.027 \times 10^{-6} \text{ m N}^{-2/3} \quad \text{sph. anvil} \quad (32)$$

Using these constants in solving for $F(t)$, it was found that the duration of the impulse t_d was approximately 0.2 msec for both types of anvil, which was an order of magnitude smaller than the contact times measured by Birch and Brocklehurst [2]. The theoretical and experimental force functions for a typical beam are compared in Fig. 2. If allowance is made for energy losses on impact, see Section 5, the predicted magnitude of the maximum force is only approximately half that observed, being similar to that of the initial inertial peak of the experimental curve. The fact that the predicted duration of the force is also similar to the duration of the initial peak is thought to be fortuitous. In view of the large discrepancy between the theoretical and experimental functions, the value of the Hertz constant, k was taken to be an adjustable parameter.

Fig. 3 shows the variation in calculated t_d with increasing k . It can be seen that a value of k some three or four times larger than the values from Equations 31 and 32 gave a time duration in reasonable agreement with the experimental results. The larger values of k were used in all subsequent calculations. The difference in t_d obtained for the two anvil geometries was at most 5 to 7%, and hence was neglected.

The need to increase k to obtain a fit to experiment implies from Equation 2

$$\alpha = kF^{2/3}$$

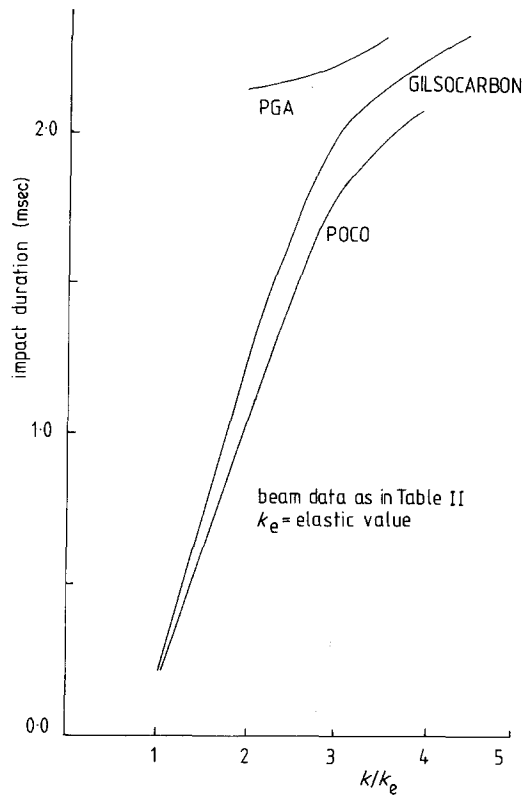


Figure 3 Variation of contact time with Hertz constant for beams.

that the depth of the indentation produced by the anvil is greater for a given force than Hertzian theory would suggest. This could be explained in terms of elastic behaviour if the effective Young's modulus of the graphite under the conditions at impact was smaller than the low strain value employed in the *ab initio* calculation of k . While this may be true qualitatively, it is difficult to justify theoretically the magnitude of the increase in k required. It must be assumed that the larger k value is the best representation within the Hertz model of the plastic deformation at the point of impact.

The effect of increasing k on the maximum value of the calculated force F_m is illustrated in Fig. 4, and it can be seen that F_m decreases for larger values of k . This is consistent with the assumption that the processes are perfectly elastic, because the impulse then depends only on the impactor's mass m and velocity v_0 , and, is a constant for a given experiment. Hence as t_d increases it is expected that F_m decreases. The experimental work [2] showed that the impact was far from being elastic, the coefficient of

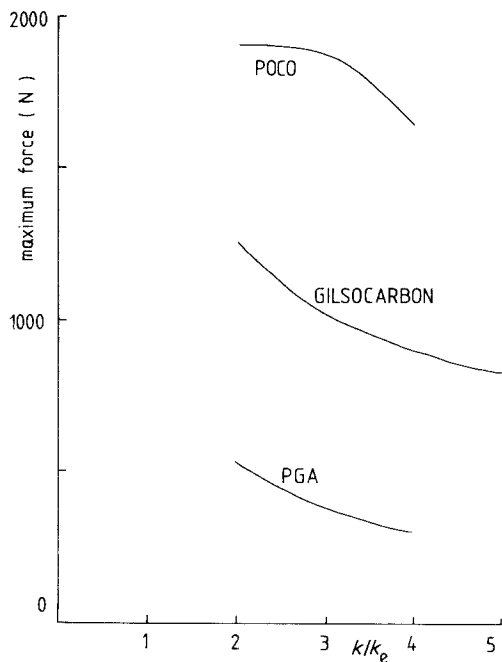


Figure 4 Maximum impact force as a function of Hertz constant for beams.

restitution being approximately 0.7. This suggests that the calculated impulse, and hence the calculated F_m , was too high by a factor 0.85.

A comparison between an experimental and theoretical force profile is shown in Fig. 5. The areas under the two curves are approximately in the ratio 1/0.85, as expected, but it is clear that the theoretical $F(t)$ cannot simply be scaled by a constant to give the experimental curves. The maximum forces are in the ratio 1/0.7. Given the uncertainties in the energy losses, the shape of the theoretical curve agrees reasonably well with experiment. The predicted oscillations, which are due to the vibrational response of the beam, are less damped at the later times. The higher fre-

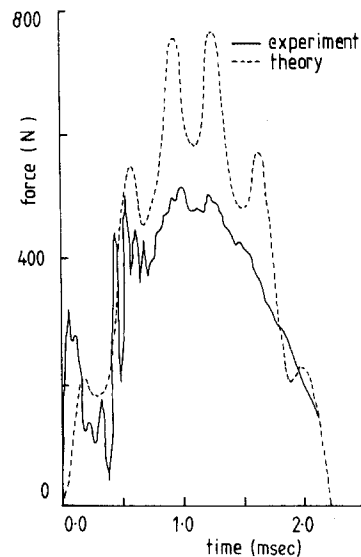


Figure 5 Impact force function for a gilsocarbon beam; (length 99 mm, radius 7.5 mm, impactor mass 0.289 kg, impact velocity 1.31 m sec^{-1}). Optimum Hertz constant used in theory.

quency components in the experimental results at earlier times may be due to vibrations of the anvil.

Calculations were also made on beams of different graphites, and a comparison of some of the theoretical and observed parameters is made in Table II.

The displacements and stresses in the beam as functions of time were calculated from a knowledge of the impulsive force. The deflection of the midpoint of the beam is given by Equation 10:

$$w_1(t) = -\frac{2}{A\rho L} \sum_{i \text{ odd}} \left\{ \frac{1}{\omega_i} \times \int_0^t F(t') \sin \left[\left(\frac{i\pi c}{L} \right)^2 (t-t') \right] dt' \right\} \quad (33)$$

TABLE II Results for beam specimens

Graphite	PGA	EY9106	Gilsocarbon	POCO
Impactor velocity, v_0 (m sec^{-1})	0.5	0.7	1.1	2.2
Contact time, t_d (msec)				
{ theory	2.40	2.93	2.27	2.07
{ expt.	2.9	2.7	2.4	2.1
Maximum force F_m (N)				
{ theory	304	378	752	1628
{ expt.	136	220	430	1000
Maximum calculated stresses (MN m^{-2})	21.4	24.7	50.1	108.8
Maximum displacement (mm)				
{ theory	0.22	0.46	0.53	1.06
{ expt.	0.5	0.6	0.9	1.5

Specimen support separation $L = 99 \text{ mm}$
 Radius of rod $r = 7.5 \text{ mm}$
 Effective mass of impactor $m = 0.289 \text{ kg}$
 Radius of anvil (spherical) $\approx 2.0 \text{ mm}$.

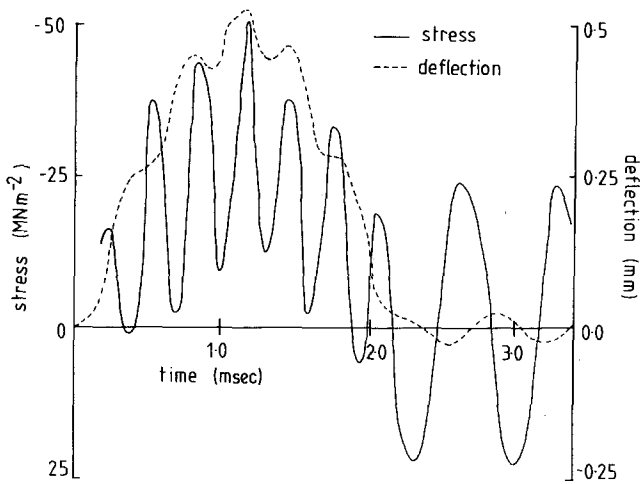


Figure 6 Calculated stress and deflection for a gilsocarbon beam (beam data as in Fig. 5).

The maximum tensile stress, in an outer fibre was determined from $\sigma_0 = -Er(\partial^2 w_1/\partial x^2)$, i.e.

$$\sigma_0 = \frac{2Er}{A\rho Lc^2} \times \sum_{i \text{ odd}} \int_0^t F(t') \sin \left[\left(\frac{inc}{L} \right)^2 (t-t') \right] dt' \quad (34)$$

The constant c is defined by Equation 19, r is the beam radius and $A = \pi r^2$. Since $F(t)$ is only known numerically, the time integrals were evaluated using the Fourier analysis method.

The rates of convergence of the two series in Equations 33 and 34 are markedly different. For the displacement the terms decrease with the eigen frequency ω_i as ω_i^{-1} , and satisfactory results were obtained with fewer than 30 terms. The terms in the summation for the stress decrease very slowly with increasing ω_i and it is essential to include as many terms as possible. In practice the largest number of terms employed was 300.

Typical calculated results for the behaviour of

the displacement $w_1(L/2, t)$ and stress in an outer fibre $\sigma_m(t)$ are illustrated in Fig. 6. The displacement appears to follow the force function for $t < t_d$, whereas the stress is clearly an oscillatory function of time. At times greater than the duration of the impact, both the displacement and stress vary harmonically.

Values of the maximum displacement were calculated for beams of four different graphites, and were compared with experimental values [2], see Table II. No allowance was made for energy losses in obtaining the theoretical values, so these are upper bounds. Even so, it is clear that they are smaller than the measured displacements by a substantial factor. This discrepancy could be due to experimental effects, such as indentation or shearing of the specimen at the supports.

Of particular interest were results for the calculated maximum stresses produced in single impact failure. The velocities v_{01} of the anvil required to cause failure were measured by Birch and Brocklehurst [1, 2], and are given in Table III for four

TABLE III Theoretical results for single impact failure of beams

Graphite	PGA	EY9106	Gilsocarbon	POCO
Length of rod, L (mm)	150	120	150	120
Impactor velocity, v_0^* (m sec $^{-1}$)	0.7	1.1	1.5	3.1
Coefficient of restitution, e^*	0.6	0.8	0.8	0.7
Contact time, t_d (msec) †	2.8	2.9	2.2	1.7
Max force, F_m (N)	327	429	775	2220
Maximum displacement (mm)	0.58	0.80	1.29	1.57
Maximum stress, σ_m (MN m $^{-2}$)	25.0	29.2	53.8	141.0
$e\sigma_m$ (MN m $^{-2}$)	15.6	23.4	43.0	98.7
Three-point bend strength, σ_b (MN m $^{-2}$)	16.4	25.8	44.0	96.0

* Estimated experimental value.

† Value if failure had not occurred. Rod radius $r = 7.5$ mm. Effective impactor mass $m = 0.289$ kg. Radius of anvil (cylindrical) 2.0 mm.

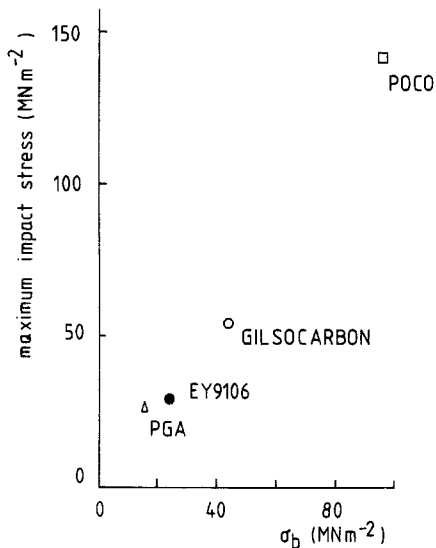


Figure 7 Variation of calculated maximum stress in beams for single impact failure as a function of the three-point bend strength.

graphites. The corresponding theoretical maximum stresses in the beams are also shown, and can be compared with the three-point bend strengths. The data are plotted in Fig. 7, and it can be seen that the maximum stresses correlate well with the three-point bend strengths. If allowance is made for energy losses by decreasing the maximum stresses by an appropriate factor, e.g. 0.7, the calculated maximum stresses at failure are essentially equal to the bend strengths; see Table III.

5. Discussion

The main defect of the theory [12, 14] used here is that the treatment of the local deformation using the Hertz formula assumes elastic bodies, and it is also based on static loading conditions. The present calculations have shown that the Hertz theory works reasonably well for graphite, provided that the single constant, k , involved is regarded as an adjustable parameter. Modifications to the theory to include plastic deformation and permanent indentation were considered by Barnhart and Goldsmith [14], but at least three adjustable parameters were required, leading to considerable complexity in fitting experimental data without much gain in understanding the physical processes involved. In general, it would be expected that the deformation constant depends on impact velocity, but this has not been considered.

A difficulty encountered in solving the integral

equation for the force function $F(t)$ was that the contact time depended sensitively on the deformation parameter k , and it was essential that experimental results for $F(t)$ were available to determine k . It was found that the best value of k was four times larger than predicted by Hertz theory, and this gives some indication of the deviation of the local properties of graphite from perfectly elastic behaviour. The resulting theoretical force functions for beams were in reasonably good agreement with experiment regarding duration and shape. However, the predicted maximum force was higher than experiment, because the theory was unable to account for energy losses.

It is only possible to discuss the energy losses in a qualitative manner. If it is assumed that the loss is proportional to the coefficient of restitution, the predicted maximum stresses at failure are equal to the static three-point bend strengths of the graphite considered, as can be seen from Table III. This result is the same as that obtained by Birch and Brocklehurst [2], using a static load model, and is of interest to compare the two approaches. In the static load case, the maximum stress is related to the maximum load by the relationship $\sigma_m = F_m L / \pi r^3$. This method is not expected to yield reliable values for F_m , and Birch and Brocklehurst used their experimental values of the force at failure to estimate σ_m . By employing these values, information is included regarding both the vibrational response of a rod and the energy loss. Since it is known from experiment, and the present calculations, that the deflection of a rod closely follows the impact force as a function of time. It can be envisaged that a static force–stress relationship may be satisfactory in this case.

6. Conclusions

The theory proposed by Hertz, with an adjustable deformation parameter combined with the mode summation method, has been used to calculate the impact force function, maximum displacements and maximum stresses in graphite beam specimens. It was found that the deformation parameter was appreciably larger than predicted by linear elastic theory.

Good agreement was obtained between theoretical and experimental force–time functions when allowance was made for the neglect of energy losses in the theory.

Calculations for beams gave results for the

maximum displacements which were smaller than experimental values. The predicted peak tensile stresses corresponding to conditions of single impact failure were found to be proportional to the static three-point bend strengths of the graphites considered.

Acknowledgements

The author thanks Dr M. Birch and Mr J. E. Brocklehurst for many helpful discussions on their experiments, and Mr B. T. Kelly for helpful suggestions. The author acknowledges financial support from the UKAEA, Northern Division.

References

1. M. BIRCH and J. E. BROCKLEHURST, An Investigation of the Impact Properties of Graphite, in "Extended abstracts of The 15th Carbon Conference", Philadelphia, June 1981 (American Carbon Society and University of Pennsylvania, 1981) p. 506.
2. *Idem*, *Carbon* **21** (1983) 497.
3. J. E. BROCKLEHURST, *Chem. Phys. Carbon* **13** (1977) 145.

4. S. TIMOSHENKO, *Zeit. Math. Physik* **62** (1913) 198.
5. S. TIMOSHENKO and D. H. YOUNG, "Vibration Problems in Engineering", 3rd edn. (Van Nostrand, London, 1955).
6. H. HERTZ, *J. Math. (Crelle)* **92** (1881) 156.
7. A. E. H. LOVE, "A Treatise on the Mathematical Theory of Elasticity", 4th edn. (Dover Publications, New York, 1944) pp. 193-200.
8. G. M. JENKINS, *Chem. Phys. Carbon* **2** (1973) 189.
9. D. R. IRELAND, "Procedures and Problems Associated with Reliable Control of the Instrumental Impact Test", ASTM Special Technical Publication 563 (1973) p. 3.
10. H. HOLZER, *Z. Ang. Math. Mech.* **4** (1928) 272.
11. K. SEZAWA, *ibid.* **5** (1932) 275.
12. W. GOLDSMITH, "Impact; the theory and physical behaviour of colliding solids", (Arnold, London 1960).
13. A. C. ERINGEN, *J. Appl. Mech.* **20** (1953) 461.
14. K. E. BARNHART and W. GOLDSMITH, *ibid.* **24** (1951) 440.

*Received 10 June
and accepted 21 September 1983*